Robotica (2006) volume 24, pp. 463–476. © 2006 Cambridge University Press
doi:10.1017/S026357470500247X Printed in the United Kingdom

Passive coordination of nonlinear bilateral teleoperated manipulators*

M. McIntyre†, W. Dixon‡, D. Dawson† and E. Tatlicioglu†

(Received in Final Form: September 20, 2005. First published online: January 3, 2006)

SUMMARY

Significant research has been aimed at the development and control of teleoperator systems due to both the practical importance and the challenging theoretical nature of the problem. Two controllers are developed in this paper for a nonlinear teleoperator system that target coordination of the master and slave manipulators and passivity of the overall system. The first controller is proven to yield a semi-global asymptotic result in the presence of parametric uncertainty in the master and slave manipulator dynamic models. The second controller yields a global asymptotic result despite unmeasurable user and environmental input forces. To develop each controller, a transformation encodes the coordination and passivity objectives in the closed loop system. The coordinated system is forced to track a dynamic system to assist in meeting all control objectives. Finally, continuous nonlinear integral feedback terms are used to accommodate for incomplete system knowledge for both controllers. Lyapunov-based techniques are used to prove that all control objectives are met and that all signals are bounded.

KEYWORDS: Teleoperated manipulators; Passive coordination; Controllers.

I. INTRODUCTION

A teleoperator system consists of a user interacting with some type of input device (i.e. a master manipulator) with the intention of imparting a predictable response by an output system (i.e. a slave manipulator). Significant research has been aimed at the development and control of teleoperator systems due to both practical importance and the challenging theoretical nature of this human-robot interaction problem. Practical applications of teleoperation are motivated by the need for task execution in hazardous environments (e.g. contaminated facilities, space, underwater), the need for remote manipulation due to the characteristics of the object (e.g. size and mass of an object, hazardous nature of the object), or the need for precision beyond human capacity (e.g. robotic assisted medical procedures). The teleoperator problem is theoretically challenging due to issues that impact the user's ability to impart a desired motion and a desired force on the remote environment through the coupled master-slave system. Some difficult issues include the presence of uncertainty in the master and slave dynamics, the ability to model accurately or measure environmental and user inputs to the system, the ability to safely reflect desired forces back to the user while mitigating other forces, and the stability of the overall system (e.g. as stated in Lee *et al.*,[1] a stable teleoperator system may be destabilized when interacting with a stable environment due to coupling between the systems).

The emphasis of some previous related research is to achieve ideal transparency by exactly transferring the slave robot impedance to the user. Typically, approaches that aim for ideal transparency either require *a priori* knowledge of the environmental inputs to the slave manipulator, as in Colgate *et al.*,[2] or estimate the impedance of the slave manipulator.[3] Some exceptions include the teleoperator controllers aimed at low-frequency transparency[4,5] that do not require knowledge of the impedance of the user or environment. However, the approaches in Colgate *et al.*,[2] Hannaford *et al.*,[3] Lawrence *et al.*,[4] and Salcudean *et al.*,[5] are based on linear teleoperator systems with frequency-based control designs. A review of other frequency-based approaches applied to linear teleoperator systems are given in citations.[6–10] In Hung *et al.*,[11] an adaptive nonlinear control design is presented that achieves transparency in the sense of motion and force tracking.

Other research has emphasized the stability and safe operation of the teleoperator system through passivity concepts.[1,6,12–18] In Anderson *et al.*,[6] Anderson and Spong used passivity and scattering criterion to propose a bilateral control law for a linear time-invariant teleoperator system in any environment and in the presence of time delay. These results were then extended with the use of wave-variables to define a new configuration for force-reflecting teleoperators.[17,18] These methods where extended to solve the position tracking problem.[12,13,18] In Lee *et al.*,[1] a passivity-based approach was used to develop a controller that renders a linear teleoperator system as a passive rigid mechanical tool with desired kinematic and power scaling capabilities. The development in Lee *et al.*,[1] was extended to nonlinear teleoperator systems.[14,15] These controllers[14,15] are dependent on knowledge of the dynamics of the master and slave manipulators and force measurements.

* This work is supported in part by two DOC Grants, an ARO Automotive Center Grant, a DOE Contract, a Honda Corporation Grant, and a DARPA Contract.
† Department of Electrical & Computer Engineering, Clemson University, Clemson, SC 29634-0915 (USA).
‡ Department of Mechanical & Aerospace Engineering, University of Florida, Gainesville, FL 32611-6250 (USA).
Corresponding author: M. McIntyre; E-mail: mmcinty@clemson.edu

In comparison to the previous literature, two controllers are developed in this paper for nonlinear teleoperator systems that target coordination of the master and slave manipulators as well as passivity of the overall system. The first controller is proven to yield a semi-global asymptotic result in the presence of parametric uncertainty in the master and slave manipulator dynamic models provided the user and environmental input forces are measurable; henceforth, referred to as the MIF (measurable input force) controller. The second controller yields a global asymptotic result despite unmeasurable user and environmental input forces (UMIF) provided the dynamic models of the respective manipulators are known. The novelty in developing each controller resided in the three following steps. The first utilizes a transformation which encodes both the coordination and passivity objectives within the closed loop system. Next, a dynamic trajectory generating system is designed which assists in achieving overall system passivity as well as keeping all signals bounded in the closed loop system. Finally, a continuous nonlinear integral feedback observer[19,20] is exploited to compensate for the lack of system dynamics information or user and environmental force measurements. For each controller, Lyapunov-based techniques are used to prove that these three steps develop a stable passively coordinated teleoperator system.

The controllers developed in this work utilize the nonlinear dynamic model which offers a clear advantage over past results for linear teleoperator systems.[2–5] The MIF controller developed in Section III compensates for unknown system parameters, which offers an improvement over past works that require exact model knowledge.[2,3] The UMIF controller developed in Section IV compensates for unavailable force measurement, which offers an improvement over works that requires force measurements.[14,15] Numerical simulation results are presented for each controller in Sections III.4 and IV.4, respectively.

II. SYSTEM MODEL

The dynamic model for a $2n$-DOF nonlinear teleoperator consisting of a revolute n-DOF master and a revolute n-DOF slave revolute robot are described by the following expressions[14]

$$\gamma\{M_1(q_1(t))\ddot{q}_1(t) + C_1(q_1(t), \dot{q}_1(t))\dot{q}_1(t) + B_1\dot{q}_1(t) = T_1(t) + F_1(t)\} \quad (1)$$

$$M_2(q_2(t))\ddot{q}_2(t) + C_2(q_2(t), \dot{q}_2(t))\dot{q}_2(t) + B_2\dot{q}_2(t) = T_2(t) + F_2(t). \quad (2)$$

In (1) and (2), $\gamma \in \mathbb{R}$ denotes a positive adjustable power scaling term, $q_i(t), \dot{q}_i(t), \ddot{q}_i(t) \in \mathbb{R}^n$ denote the link position, velocity, and acceleration, respectively, $\forall i = 1, 2$ where $i = 1$ denotes the master manipulator and $i = 2$ denotes the slave manipulator, $M_i(q_i) \in \mathbb{R}^{n\times n}$ represents the inertia effects, $C_i(q_i, \dot{q}_i) \in \mathbb{R}^{n\times n}$ represents centripetal-Coriolis effects, $B_i \in \mathbb{R}^{n\times n}$ represents the constant positive definite, diagonal dynamic frictional effects, $T_i(t) \in \mathbb{R}^n$ represents the torque input control vector, $F_1(t) \in \mathbb{R}^n$ represents the user input force, and $F_2(t) \in \mathbb{R}^n$ represents the input force from the environment. The subsequent development is based on the property that the master and slave inertia matrices are positive definite and symmetric in the sense that[21]

$$m_{1i}\|\xi\|^2 \le \xi^T M_i(q_i)\xi \le m_{2i}\|\xi\|^2 \ \forall \xi \in \mathbb{R}^n \text{ and } i = 1, 2 \quad (3)$$

where $m_{1i}, m_{2i} \in \mathbb{R}$ are positive constants, and $\|\cdot\|$ denotes the Euclidean norm. The subsequent development is also based on the assumption that $q_i(t)$, $\dot{q}_i(t)$ are measurable, and that the inertia and centripetal-Coriolis matrices are second order differentiable.

III. MIF CONTROL DEVELOPMENT

For the MIF controller development, the subsequent analysis will prove a semi-global asymptotic result in the presence of parametric uncertainty in the master and slave manipulator dynamic models provided the user and environmental input forces are measurable. This development requires the assumption that $F_i(t)$, $\dot{F}_i(t)$, $\ddot{F}_i(t) \in L_\infty$ $\forall i = 1, 2$ (precedence for this type of assumption is provided in references [1 and 14]).

III.1. Objective and model transformation

One of the two primary objectives for the bilateral teleoperator system is to ensure coordination between the master and the slave manipulators in the following sense

$$q_2(t) \to q_1(t) \text{ as } t \to \infty. \quad (4)$$

The other primary objective is to ensure that the system remains passive with respect to the scaled user and environmental power in the following sense[14]

$$\int_{t_0}^{t} \left(\gamma \dot{q}_1^T(\tau)F_1(\tau) + \dot{q}_2^T(\tau)F_2(\tau)\right) d\tau \ge -c_1^2 \quad (5)$$

where $c_1 \in \mathbb{R}$ is a bounded positive constant, and γ was introduced in (1). The passivity objective is included in this section to ensure that the human can interact with the robotic system in a stable and safe manner, and that the robot can also interact with the environment in a stable and safe manner. To facilitate the passivity objective in (5), an auxiliary control objective is utilized. Specifically, the coordinated master and slave manipulators are forced to track a desired bounded trajectory, denoted by $q_d(t) \in \mathbb{R}^n$, in the sense that[15]

$$q_1(t) + q_2(t) \to q_d(t). \quad (6)$$

An additional objective is that all signals are required to remain bounded within the closed loop system.

To facilitate the subsequent development, a globally invertible transformation is defined that encodes both the coordination and passivity objectives as follows

$$x \triangleq Sq \quad (7)$$

https://doi.org/10.1017/S026357470500247X Published online by Cambridge University Press

where $x(t) \triangleq [x_1^T(t)\, x_2^T(t)]^T \in \mathbb{R}^{2n}$, $q(t) \triangleq [q_1^T(t)\, q_2^T(t)]^T \in \mathbb{R}^{2n}$, and $S \in \mathbb{R}^{2n\times 2n}$ is defined as follows

$$S \triangleq \begin{bmatrix} I & -I \\ I & I \end{bmatrix} \quad S^{-1} = \frac{1}{2}\begin{bmatrix} I & I \\ -I & I \end{bmatrix} \tag{8}$$

where $I \in \mathbb{R}^{n\times n}$ denotes the identity matrix. Based on (7), the dynamic models given in (1) and (2) can be expressed as follows

$$\bar{M}(x)\ddot{x} + \bar{C}(x,\dot{x})\dot{x} + \bar{B}\dot{x} = \bar{T}(t) + \bar{F}(t) \tag{9}$$

where

$$\bar{M}(x) = S^{-T}\begin{bmatrix} \gamma M_1 & 0_{2n} \\ 0_{2n} & M_2 \end{bmatrix} S^{-1} \in \mathbb{R}^{2n\times 2n} \tag{10}$$

$$\bar{C}(x,\dot{x}) = S^{-T}\begin{bmatrix} \gamma C_1 & 0_{2n} \\ 0_{2n} & C_2 \end{bmatrix} S^{-1} \in \mathbb{R}^{2n\times 2n} \tag{11}$$

$$\bar{B} = S^{-T}\begin{bmatrix} \gamma B_1 & 0_{2n} \\ 0_{2n} & B_2 \end{bmatrix} S^{-1} \in \mathbb{R}^{2n\times 2n} \tag{12}$$

$$\bar{T}(t) = S^{-T}\begin{bmatrix} \gamma T_1^T & T_2^T \end{bmatrix}^T \in \mathbb{R}^{2n} \tag{13}$$

$$\bar{F}(t) \triangleq \begin{bmatrix} \bar{F}_1(t) \\ \bar{F}_2(t) \end{bmatrix} = S^{-T}\begin{bmatrix} \gamma F_1 \\ F_2 \end{bmatrix} \in \mathbb{R}^{2n} \tag{14}$$

and $0_{2n} \in \mathbb{R}^{n\times n}$ denotes an $n \times n$ matrix of zeros. The subsequent development is based on the property that $\bar{M}(x)$, as defined in (10), is a positive definite and symmetric matrix in the sense that[21]

$$\bar{m}_1\|\xi\|^2 \le \xi^T\bar{M}(x)\xi \le \bar{m}_2\|\xi\|^2 \ \forall \xi \in \mathbb{R}^{2n} \tag{15}$$

where $\bar{m}_1, \bar{m}_2 \in \mathbb{R}$ are positive constants. It is also noted that $\bar{M}(x)$ is second order differentiable by assumption.

To facilitate the subsequent development and analysis, the control objectives can be combined through a filtered tracking error signal, denoted by $r(t) \in \mathbb{R}^{2n}$, that is defined as follows

$$r \triangleq \dot{e}_2 + \alpha_1 e_2 \tag{16}$$

where $e_2(t) \in \mathbb{R}^{2n}$ is defined as follows

$$e_2 \triangleq \dot{e}_1 + \alpha_2 e_2 \tag{17}$$

where $\alpha_1, \alpha_2 \in \mathbb{R}$ are positive control gains, and $e_1(t) \in \mathbb{R}^{2n}$ is defined as follows

$$e_1 \triangleq x_d - x \tag{18}$$

where $x_d(t) \in \mathbb{R}^{2n}$ is defined as follows

$$x_d \triangleq \begin{bmatrix} 0_n^T & q_d^T(t) \end{bmatrix}^T \tag{19}$$

where $0_n \in \mathbb{R}^n$ denotes an $n \times 1$ vector of zeros. Based on the definition of $x(t)$ in (7) and $e_1(t)$ in (18), it is clear that if $\|e_1(t)\| \to 0$ as $t \to \infty$ then $q_2(t) \to q_1(t)$ and that $q_1(t) + q_2(t) \to q_d(t)$ as $t \to \infty$.

The desired trajectory $q_d(t)$ introduced in (6) and (19) is generated by the following expression

$$M_T\ddot{q}_d + B_T\dot{q}_d + K_T q_d = \bar{F}_2. \tag{20}$$

In (20), M_T, B_T, $K_T \in \mathbb{R}^{n\times n}$ represent constant positive definite, diagonal matrices, and $\bar{F}_2(t)$ was introduced in (14). Based on the assumption that $\bar{F}_2(t) \in \mathcal{L}_\infty$, standard linear analysis techniques can be used to prove that $q_d(t)$, $\dot{q}_d(t)$, $\ddot{q}_d(t) \in \mathcal{L}_\infty$. The time derivative of (20) is given by the following expression

$$M_T\dddot{q}_d + B_T\ddot{q}_d + K_T\dot{q}_d = \dot{\bar{F}}_2. \tag{21}$$

From (21), the fact that $\dot{q}_d(t), \ddot{q}_d(t) \in \mathcal{L}_\infty$, and the assumption that $\dot{\bar{F}}_2(t) \in \mathcal{L}_\infty$, it is clear that $\dddot{q}_d(t) \in \mathcal{L}_\infty$. By taking the time derivative of (21), and utilizing the assumption that $\ddot{\bar{F}}_2(t) \in \mathcal{L}_\infty$, hence, it can be proven that $\ddddot{q}_d(t) \in \mathcal{L}_\infty$.

III.2. Closed-loop error system

Based on the assumption that the user and environmental forces are measurable, the control input $\bar{T}(t)$ of (13) is designed as follows

$$\bar{T} \triangleq \bar{u} - \bar{F} \tag{22}$$

where $\bar{u}(t) \in \mathbb{R}^{2n}$ is an auxiliary control input. Substituting (22) into (9) yields the following simplified system

$$\bar{M}\ddot{x} + \bar{C}\dot{x} + \bar{B}\dot{x} = \bar{u}. \tag{23}$$

After taking the time derivative of (16) and premultiplying by $\bar{M}(x)$, the following expression can be obtained

$$\bar{M}\dot{r} = \bar{M}\,\dddot{x}_d + \dot{\bar{M}}\ddot{x} + \frac{d}{dt}[\bar{C}\dot{x} + \bar{B}\dot{x}] - \dot{\bar{u}} + \alpha_2\bar{M}\ddot{e}_1 + \alpha_1\bar{M}\dot{e}_2 \tag{24}$$

where (16)–(18), and the time derivative of (23) were utilized. To facilitate the subsequent analysis, the expression in (24) is rewritten as follows

$$\bar{M}\dot{r} = \tilde{N} + N_d - e_2 - \dot{\bar{u}} - \frac{1}{2}\dot{\bar{M}}r \tag{25}$$

where the auxiliary signal $\tilde{N}(x,\dot{x},\ddot{x},t) \in \mathbb{R}^{2n}$ is defined as

$$\tilde{N} \triangleq N - N_d \tag{26}$$

where $N(x,\dot{x},\ddot{x},t) \in \mathbb{R}^{2n}$ is defined as

$$N \triangleq \bar{M}\,\dddot{x}_d + \dot{\bar{M}}\ddot{x} + \alpha_2\bar{M}\ddot{e}_1 + \alpha_1\bar{M}\dot{e}_2 + e_2 + \frac{d}{dt}[\bar{C}\dot{x} + \bar{B}\dot{x}] + \frac{1}{2}\dot{\bar{M}}r \tag{27}$$

and $N_d(t) \in \mathbb{R}^{2n}$ is defined as

$$N_d \triangleq N|_{x=x_d,\dot{x}=\dot{x}_d,\ddot{x}=\ddot{x}_d} = \bar{M}(x_d)\,\dddot{x}_d + \dot{\bar{M}}(x_d,\dot{x}_d)\ddot{x}_d + \frac{d}{dt}[\bar{C}(x_d,\dot{x}_d)\dot{x}_d + \bar{B}\dot{x}_d]. \tag{28}$$

https://doi.org/10.1017/S026357470500247X Published online by Cambridge University Press

Remark 1. *To facilitate the subsequent analysis, the following upper bound can be developed for* $\tilde{N}\cdot$

$$\|\tilde{N}\| \leq \rho(\|z\|)\|z\| \quad \textit{where } z \triangleq \begin{bmatrix} e_1^T & e_2^T & r^T \end{bmatrix}^T$$

and the positive function $\rho(\|z\|)$ *is non-decreasing in* $\|z\|$ (*see McIntyre* et al.[22] *for further details*).

Based on (25), the auxiliary control input $\bar{u}(t)$ introduced in (22) is designed as follows

$$\bar{u} \triangleq (k_s+1)\left[e_2(t) - e_2(t_0) + \alpha_1 \int_{t_0}^{t} e_2(\tau)\, d\tau\right] + (\beta_1+\beta_2)\int_{t_0}^{t} sgn(e_2(\tau))\, d\tau \tag{29}$$

where $k_s, \beta_1, \beta_2 \in \mathbb{R}$ are positive control gains, and $sgn(\cdot)$ denotes the vector signum function. The term $e_2(t_0)$ in (29) is included to provide that $\bar{u}(t_0) = 0$. The time derivative of (29) is given by the following expression

$$\dot{\bar{u}} = (k_s+1)r + (\beta_1+\beta_2)\, sgn(e_2). \tag{30}$$

Substituting (30) into (25) yields the following closed-loop error system

$$\bar{M}\dot{r} = -(k_s+1)r - (\beta_1+\beta_2)\, sgn(e_2) + \tilde{N} + N_d - e_2 - \frac{1}{2}\dot{\bar{M}}r. \tag{31}$$

Remark 2. *Based on the expressions in* (19), (28) *and the fact that* $q_d(t), \dot{q}_d(t), \ddot{q}_d(t)$, *and* $\dddot{q}_d(t) \in \mathcal{L}_\infty$, *then* $\|N_d(t)\|$ *and* $\|\dot{N}_d(t)\|$ *can be upper bounded by known positive constants* $\varsigma_1, \varsigma_2 \in \mathbb{R}$ *as follows*

$$\|N_d(t)\| \leq \varsigma_1 \quad \|\dot{N}_d(t)\| \leq \varsigma_2. \tag{32}$$

III.3. Stability analysis

Theorem 1. *The controllers given in* (22) *and* (29), *ensure that all closed-loop signals are bounded and that coordination between the master and slave manipulators is achieved in the sense that*

$$q_2(t) \to q_1(t) \quad as \quad t \to \infty \tag{33}$$

provided the control gain β_1 *introduced in* (29) *is selected to satisfy the following sufficient condition*

$$\beta_1 > \varsigma_1 + \frac{1}{\alpha_1}\varsigma_2 \tag{34}$$

where ς_1 *and* ς_2 *are given in* (32), *the control gains* α_1 *and* α_2 *are selected greater than* 2, *and* k_s *is selected sufficiently large with respect to the initial conditions of the system.*

Proof. See McIntyre *et al.*[22] for proof.

Theorem 2. *The controllers given in* (22) *and* (29), *ensure that the teleoperator system is passive with respect to the scaled user and environmental power.*

Proof. See McIntyre *et al.*[22] for proof.

III.4. Simulation results

A numerical simulation was performed to demonstrate the performance of the controllers given in (22) and (29). The following 2-link, revolute robot dynamic model was utilized for both the master and slave manipulators[23]

$$\begin{bmatrix} \tau_{i_1} \\ \tau_{i_2} \end{bmatrix} + \begin{bmatrix} F_{i_1} \\ F_{i_2} \end{bmatrix} = \begin{bmatrix} p_{1_i} + 2p_{3_i}c(q_{i_2}) + 2p_{4_i}s(q_{i_2}) & p_{2_i} + p_{3_i}c(q_{i_2}) + p_{4_i}s(q_{i_2}) \\ p_{2_i} + p_{3_i}c(q_{i_2}) + p_{4_i}s(q_{i_2}) & p_{2_i} \end{bmatrix} \begin{bmatrix} \ddot{q}_{i_1} \\ \ddot{q}_{i_2} \end{bmatrix} + \begin{bmatrix} -(p_{3_i}s(q_{i_2}) - p_{4_i}c(q_{i_2}))\dot{q}_{i_2} & -(p_{3_i}s(q_{i_2}) - p_{4_i}c(q_{i_2}))(\dot{q}_{i_1}+\dot{q}_{i_2}) \\ (p_{3_i}s(q_{i_2}) - p_{4_i}c(q_{i_2}))\dot{q}_{i_1} & 0 \end{bmatrix} \begin{bmatrix} \dot{q}_{i_1} \\ \dot{q}_{i_2} \end{bmatrix} + \begin{bmatrix} f_{d1_i} & 0 \\ 0 & f_{d2_i} \end{bmatrix} \begin{bmatrix} \dot{q}_{i_1} \\ \dot{q}_{i_2} \end{bmatrix} \tag{35}$$

where $s(\cdot)$ and $c(\cdot)$ denote the $\sin(\cdot)$ and $\cos(\cdot)$ functions. For the master manipulator, $i = 1$ and $p_{1_1} = 3.34$ [kg · m^2], $p_{2_1} = 0.97$ [kg · m^2], $p_{3_1} = 1.0392$ [kg · m^2], $p_{4_1} = 0.6$ [kg · m^2], $f_{d1_1} = 1.3$ [Nm · sec], and $f_{d2_1} = 0.88$ [Nm · sec]. For the slave manipulator, $i = 2$ and $p_{1_2} = 2.67$ [kg · m^2], $p_{2_2} = 1.455$ [kg · m^2], $p_{3_2} = 0.929$ [kg · m^2], $p_{4_2} = 0.537$ [kg · m^2], $f_{d1_2} = 1.3$ [Nm · sec], and $f_{d2_2} = 0.88$ [Nm · sec], where the parameters are based on reference [23]. For this simulation, the positive adjustable power scaling term was selected as $\gamma = 1$. The user input force vector was set equal to the following arbitrary periodic time-varying signals

$$\begin{bmatrix} F_{1_1} \\ F_{1_2} \end{bmatrix} = \begin{bmatrix} 25\sin(1.1t) \\ 35\sin(t) \end{bmatrix}. \tag{36}$$

To emulate contact with the environment, a spring-like input force vector was selected as follows

$$\begin{bmatrix} F_{2_1} \\ F_{2_2} \end{bmatrix} = \begin{bmatrix} -0.6\dot{q}_{1_2} - q_{1_2} \\ -0.6\dot{q}_{2_2} - q_{2_2} \end{bmatrix}. \tag{37}$$

To assist in meeting the passivity control objective, the coordinated teleoperated system must follow a desired trajectory which was generated by the system described by (20) and for this simulation was selected as follows

$$\bar{F}_2(t) = \begin{bmatrix} 5 & 0 \\ 0 & 5 \end{bmatrix}\begin{bmatrix} \ddot{q}_{d1} \\ \ddot{q}_{d2} \end{bmatrix} + \begin{bmatrix} 3 & 0 \\ 0 & 3 \end{bmatrix}\begin{bmatrix} \dot{q}_{d1} \\ \dot{q}_{d2} \end{bmatrix} + \begin{bmatrix} 1 & 0 \\ 0 & 1 \end{bmatrix}\begin{bmatrix} q_{d1} \\ q_{d2} \end{bmatrix} \tag{38}$$

where $q_{d1}(t)$ and $q_{d2}(t)$ denote the desired link positions, and $\bar{F}_2(t)$ is equal to the following expression

$$\bar{F}_2(t) = \frac{1}{2}(\gamma F_1(t) + F_2(t))$$

where $\bar{F}_2(t)$ was defined in (14).

The actual trajectories for the master and slave manipulators are demonstrated in Figure 1 for controller gains selected as $k_s = 100$ and $\beta_1 + \beta_2 = 25$. The link position tracking error between the master and slave manipulators

https://doi.org/10.1017/S026357470500247X Published online by Cambridge University Press

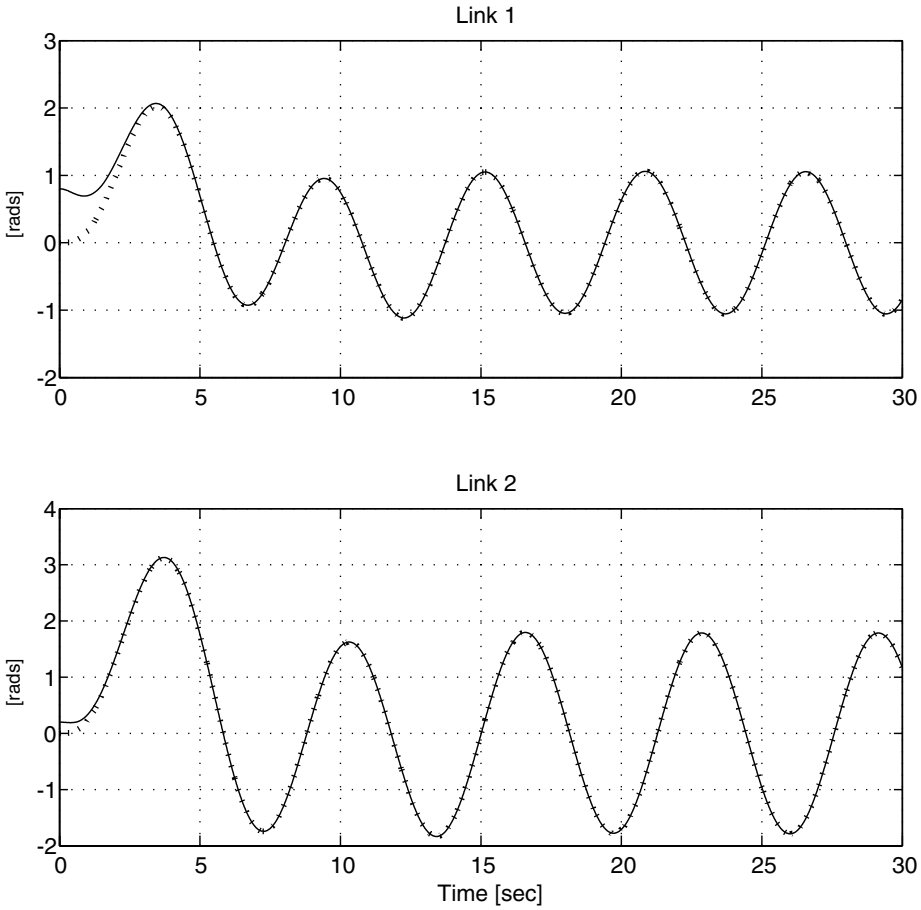

Fig. 1. Actual trajectories for master (i.e. $q_1(t)$) (—) and slave (i.e. $q_2(t)$) (- -) manipulators for Link 1 and Link 2.

can be seen in Figure 2. From Figures 1 and 2, it is clear that the coordination control objective is achieved. The actual trajectory for the coordinated system $(q_1(t) + q_2(t))$ and the desired trajectory as defined by (38), are demonstrated in Figure 3. The coordinated system versus the desired trajectory tracking error as defined by $q_1(t) + q_2(t) - q_d(t)$, is given in Figure 4. From Figures 3 and 4, it is clear that the coordinated system tracks the desired trajectory. The control torque inputs for the master and slave manipulator are provided in Figures 5 and 6, respectively.

IV. UMIF CONTROL DEVELOPMENT

For the UMIF controller development, the subsequent analysis will prove a global asymptotic result despite unmeasurable user and environmental input forces (UMIF) provided the dynamic models of the respective manipulators are known. This development also requires the assumption that $F_i(t), \dot{F}_i(t), \ddot{F}_i(t) \in L_\infty \forall i = 1, 2$.

IV.1. Objective and model transformation

One of the two primary objectives for the bilateral teleoperator system is to ensure coordination between the master and the slave manipulators as in (4). The other objective is to ensure that the system remains passive with respect to the scaled user and environmental power as in (5). To assist in meeting the passivity objective the following desired trajectory, defined as $x_d(t) \in \mathbb{R}^{2n}$, is generated by the following dynamic system

$$\bar{M}\ddot{x}_d + B_T\dot{x}_d + K_T x_d + \frac{1}{2}\dot{\bar{M}}\dot{x}_d = \hat{F}. \tag{39}$$

In (39), $\bar{M}(x)$ was defined in (10), B_T and $K_T \in \mathbb{R}^{2n\times 2n}$ represent constant positive definite, diagonal matrices, and $\hat{F}(t) \in \mathbb{R}^{2n}$ is a subsequently designed nonlinear force observer, and $x_d(t) \in \mathbb{R}^{2n}$ can be decomposed as follows

$$x_d = \begin{bmatrix} x_{d1}^T(t) & x_{d2}^T(t) \end{bmatrix}^T \tag{40}$$

where $x_{d1}(t), x_{d2}(t) \in \mathbb{R}^n$. Subsequent development will prove that $\hat{F}(t) \in \mathcal{L}_\infty$. Based on this fact, the development in Appendix C of McIntyre *et al.*[22] can be used to prove that $x_d(t), \dot{x}_d(t) \in \mathcal{L}_\infty$, then (39) can be used to prove that $\ddot{x}_d(t) \in \mathcal{L}_\infty$ as shown later, the passivity objective is facilitated by ensuring that the coordinated master and slave manipulators are forced to track a desired bounded trajectory $x_{d2}(t)$ in the sense that

$$q_1(t) + q_2(t) \to x_{d2}(t) \tag{41}$$

where $x_{d2}(t)$ was defined in (40). An additional objective is that all signals are required to remain bounded within the closed loop system.

https://doi.org/10.1017/S026357470500247X Published online by Cambridge University Press

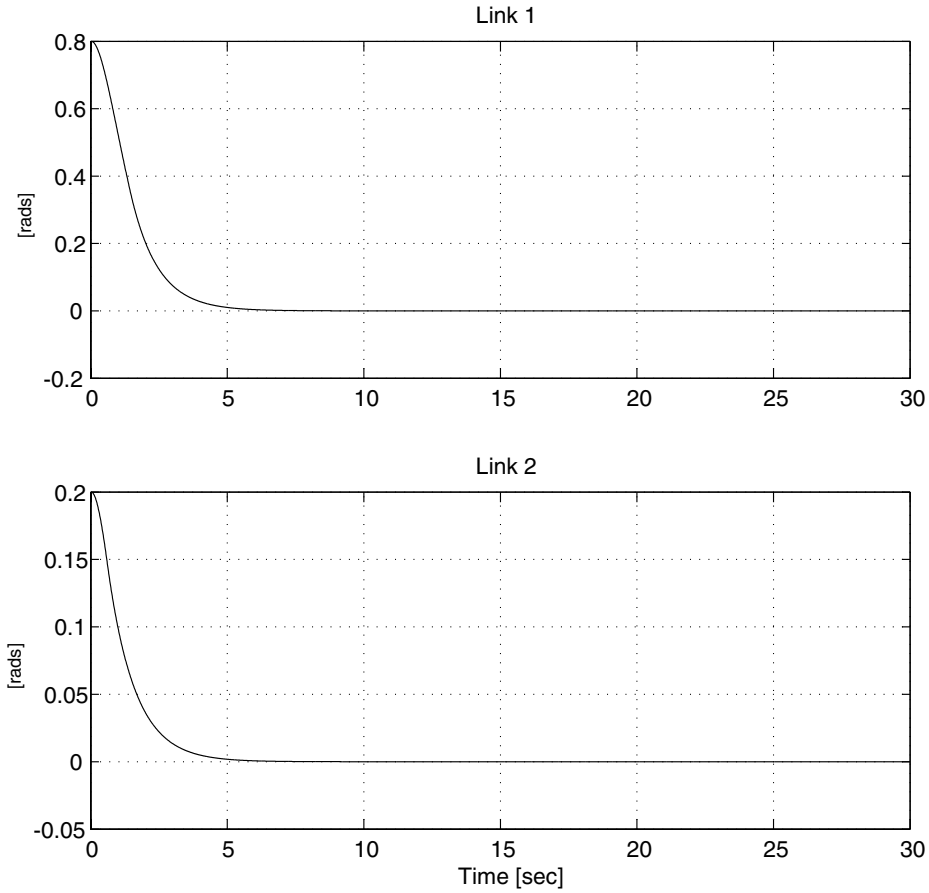

Fig. 2. Link position tracking error between the master and slave manipulators (i.e. $q_1(t) - q_2(t)$).

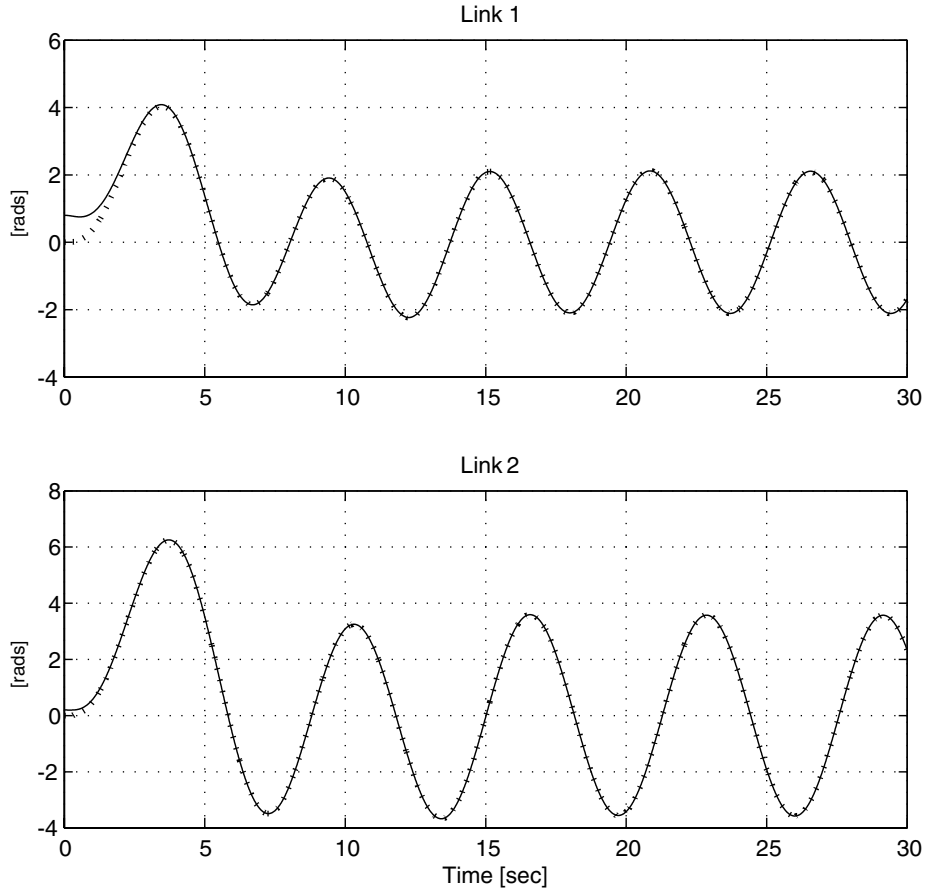

Fig. 3. Actual coordinated (i.e. $q_1(t) + q_2(t)$) trajectory (—) and desired (i.e. $q_d(t)$) trajectory (- -) for Link 1 and Link 2.

https://doi.org/10.1017/S026357470500247X Published online by Cambridge University Press

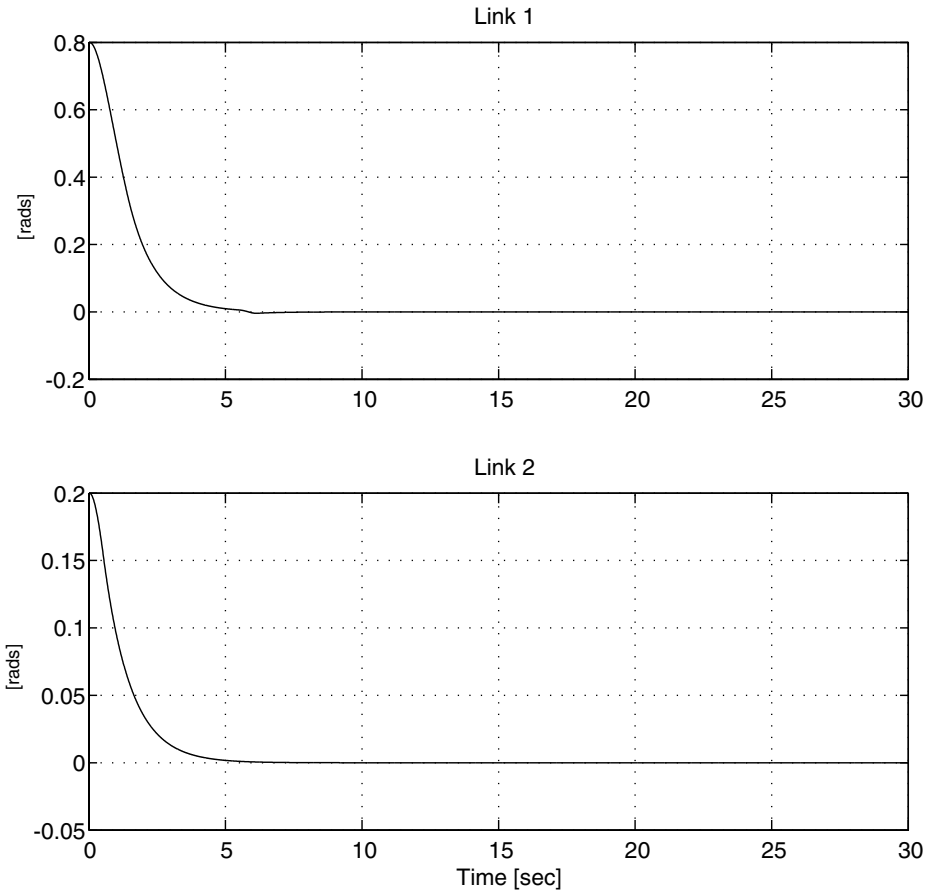

Fig. 4. The coordinated system versus the desired trajectory tracking error (i.e. $q_1(t) + q_2(t) - q_d(t)$).

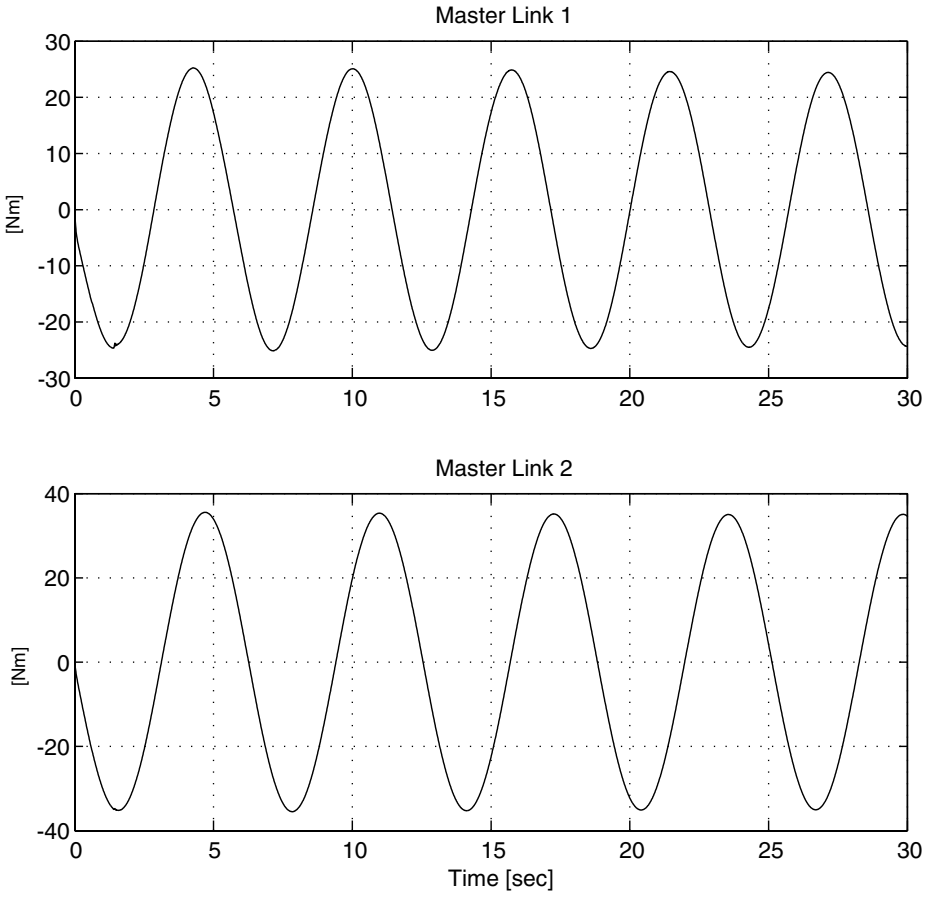

Fig. 5. Master manipulator control input torque (i.e. $\tau_1(t)$).

https://doi.org/10.1017/S026357470500247X Published online by Cambridge University Press

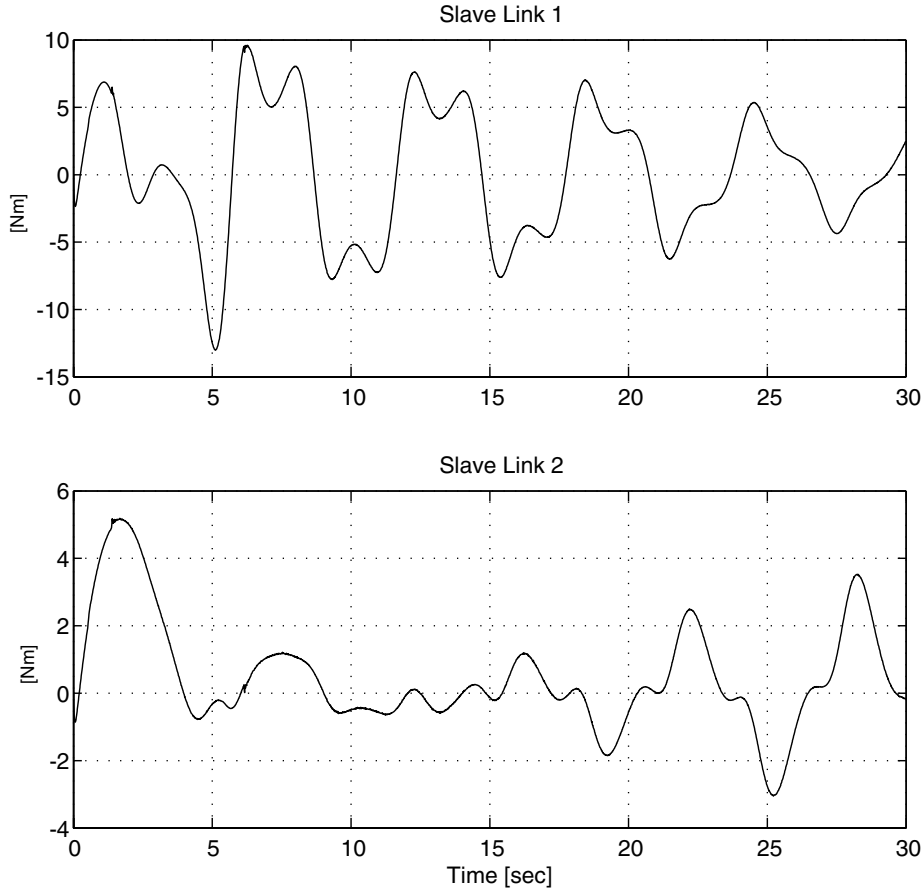

Fig. 6. Slave manipulator control input torque (i.e. $\tau_2(t)$).

To facilitate the subsequent development, a globally invertible transformation is defined that encodes both the coordination and passivity objectives as follows

$$x \triangleq Sq + \begin{bmatrix} x_{d1} \\ 0_n \end{bmatrix} \tag{42}$$

where $x(t) \triangleq [x_1^T(t)\ x_2^T(t)]^T \in \mathbb{R}^{2n}$, $q(t) \triangleq [q_1^T(t)\ q_2^T(t)]^T \in \mathbb{R}^{2n}$, $x_{d1}(t) \in \mathbb{R}^n$ was defined in (40), the zero vector $0_n \in \mathbb{R}^n$ and $S \in \mathbb{R}^{2n\times 2n}$ was defined in (8). Based on (42), the dynamic models given in (1) and (2) can be expressed as follows

$$\bar{M}(x)\ddot{x} - \bar{M}(x)\begin{bmatrix} \ddot{x}_{d1} \\ 0_n \end{bmatrix} + \bar{C}(x,\dot{x})\dot{x} - \bar{C}(x,\dot{x})\begin{bmatrix} \dot{x}_{d1} \\ 0_n \end{bmatrix} + \bar{B}\dot{x} - \bar{B}\begin{bmatrix} \dot{x}_{d1} \\ 0_n \end{bmatrix} = \bar{T}(t) + \bar{F}(t) \tag{43}$$

where $\bar{M}(x)$, $\bar{C}(x,\dot{x})$, $\bar{B}$, $\bar{T}(t)$, and $\bar{F}(t)$ were defined in (10)–(14).

To facilitate the subsequent UMIF development and analysis, the control objectives can be combined through a filtered tracking error signal denoted by $r(t) \in \mathbb{R}^{2n}$, that is defined as follows

$$r \triangleq \dot{e}_2 + e_2 \tag{44}$$

where $e_2(t) \in \mathbb{R}^{2n}$ is now defined as follows

$$e_2 \triangleq \bar{M}(\dot{e}_1 + \alpha_2 e_1) \tag{45}$$

where $\alpha_2 \in \mathbb{R}$ is a positive control gain, and $e_1(t) \in \mathbb{R}^{2n}$ was defined in (18) as follows

$$e_1 \triangleq x_d - x$$

where $x_d(t)$ was defined in (40).

IV.2. Closed loop error system

To facilitate the development of the closed-loop error system for $r(t)$, we first examine the error system dynamics for $e_1(t)$ and $e_2(t)$. To this end, we take the second time derivative of $e_1(t)$ and premultiply by $\bar{M}(x)$ to obtain the following expression

$$\bar{M}\ddot{e}_1 = \hat{F} - B_T\dot{x}_d - K_T x_d - \frac{1}{2}\dot{\bar{M}}\dot{x}_d - \bar{T} - \bar{F} - \bar{M}\begin{bmatrix} \ddot{x}_{d1} \\ 0_n \end{bmatrix} + \bar{C}\dot{x} - \bar{C}\begin{bmatrix} \dot{x}_{d1} \\ 0_n \end{bmatrix} + \bar{B}\dot{x} - \bar{B}\begin{bmatrix} \dot{x}_{d1} \\ 0_n \end{bmatrix} \tag{46}$$

where (43) and (39) were utilized. Based on the assumption of exact model knowledge, the control input $\bar{T}(t)$ is designed

https://doi.org/10.1017/S026357470500247X Published online by Cambridge University Press

as follows

$$\bar{T} \triangleq \bar{T}_1 - B_T\dot{x}_d - K_T x_d - \frac{1}{2}\dot{\bar{M}}\,\dot{x}_d - \bar{M}\begin{bmatrix}\ddot{x}_{d1}\\ 0_n\end{bmatrix} + \bar{C}\dot{x} - \bar{C}\begin{bmatrix}\dot{x}_{d1}\\ 0_n\end{bmatrix} + \bar{B}\dot{x} - \bar{B}\begin{bmatrix}\dot{x}_{d1}\\ 0_n\end{bmatrix} \tag{47}$$

where $\bar{T}_1(t) \in \mathbb{R}^{2n}$ is an auxiliary control input. Substituting (47) into (46) yields the following simplified expression

$$\bar{M}\ddot{e}_1 = \hat{F} - \bar{F} - \bar{T}_1. \tag{48}$$

Based on (48), the time derivative of $e_2(t)$ in (45) can be obtained as follows

$$\dot{e}_2 = \dot{\bar{M}}\,\dot{e}_1 + \alpha_2\dot{\bar{M}}\dot{e}_1 + \alpha_2\bar{M}\dot{e}_1 + \hat{F} - \bar{F} - \bar{T}_1. \tag{49}$$

Based on the expression in (49), the auxiliary control input $\bar{T}_1(t)$ is designed as follows

$$\bar{T}_1 \triangleq \dot{\bar{M}}\,\dot{e}_1 + \alpha_2\dot{\bar{M}}e_1 + \alpha_2\bar{M}\dot{e}_1. \tag{50}$$

After substituting (50) into (49), the following can be written

$$\dot{e}_2 = \hat{F} - \bar{F}. \tag{51}$$

Taking the time derivative of (51) yields the resulting expression

$$\ddot{e}_2 = \dot{\hat{F}} - \dot{\bar{F}}. \tag{52}$$

The following error system dynamics can now be obtained for $r(t)$ by taking the time derivative of (44)

$$\dot{r} = r - e_2 + \dot{\hat{F}} - \dot{\bar{F}} \tag{53}$$

where (44) and (52) were both utilized. Based on (53) and the subsequent stability analysis, the proportional-integral like nonlinear force observer $\hat{F}(t)$ introduced in (39) is designed as follows

$$\hat{F} \triangleq -(k_s+1)\left[e_2(t) - e_2(t_0) + \int_{t_0}^{t} e_2(\tau)\,d\tau\right] - (\beta_1+\beta_2)\int_{t_0}^{t} sgn(e_2(\tau))\,d\tau \tag{54}$$

where k_s, β_1, and $\beta_2 \in R$ are positive control gains, and $sgn(\cdot)$ denotes the vector signum function. The expression given in (54) is designed such that $\hat{F}(t_0) = 0$. The time derivative of (54) is given by the following expression

$$\dot{\hat{F}} = -(k_s+1)r - (\beta_1+\beta_2)\,sgn(e_2). \tag{55}$$

Substituting (55) into (53) yields the following closed loop error system

$$\dot{r} = -e_2 - \dot{\bar{F}} - k_s r - (\beta+\beta)\,sgn(e_2). \tag{56}$$

Remark 3. *Based on* (14) *and the assumption that* $F_i(t)$, $\dot{F}_i(t)$, $\ddot{F}_i(t) \in L_\infty \forall i = 1, 2$, *upper bounds can be developed for* $\|\dot{\bar{F}}(t)\|$ *and* $\|\ddot{\bar{F}}(t)\|$ *as follows*

$$\|\dot{\bar{F}}(t)\| \le \varsigma_3 \quad \|\ddot{\bar{F}}(t)\| \le \varsigma_4 \tag{57}$$

where ς_3, $\varsigma_4 \in \mathbb{R}$ *denote positive constants.*

IV.3. Stability analysis

Theorem 3. *The controllers given in* (47) *and* (50) *ensure that all closed-loop signals are bounded and that coordination between the master and slave manipulators is achieved in the sense that*

$$q_2(t) \longrightarrow q_1(t) \quad as \quad t \longrightarrow \infty \tag{58}$$

provided the control gain β_1, *introduced in* (54) *is selected to satisfy the sufficient condition*

$$\beta_1 > \varsigma_3 + \varsigma_4, \tag{59}$$

where ς_3 *and* ς_4 *were introduced in* (57).

Proof. See McIntyre *et al.*[22] for proof.

Theorem 4. *The controllers given in* (47) *and* (50), *ensure that the teleoperator system is passive with respect to the scaled user and environmental power.*

Proof. See McIntyre *et al.*[22] for proof.

IV.4. Simulation results

A numerical simulation was performed for the controllers given in (47) and (50). The 2-link, revolute robot dynamic model utilized in (35) was utilized for both the master and slave manipulators. The user input force vector in (36) and the environmental input force vector in (37) were also utilized.

To meet the passivity-based control objective, the coordinated teleoperated system must follow a desired trajectory, which is generated from (39) using the same parameter values for the transformed inertia matrix. The values for B_T, $K_T \in \mathbb{R}^{4\times4}$ were set to the following values

$$B_T = diag\{5, 5, 5, 5\}$$
$$K_T = diag\{25, 25, 25, 25\}$$

where B_T and K_T are both diagonal matrices.

The actual trajectories for the master and slave manipulators are demonstrated in Figure 7 where the control gains were selected as $k_s = 100$, $\beta_1 + \beta_2 = 100$, $\alpha_2 = 200$. The link position tracking error between the master and slave manipulators can be seen in Figure 8. From Figures 7 and 8, it is clear that the coordination control objective is achieved. The actual trajectory for the coordinated system $(q_1(t) + q_2(t))$ and the desired trajectory as defined in (39), are demonstrated in Figure 9. The coordinated system versus the desired trajectory tracking error as defined by $q_1(t) + q_2(t) - x_{d2}(t)$, is given in Figure 10. From Figures 9 and 10, it is clear that the coordinated system tracks the desired trajectory. The output of the nonlinear force observer

https://doi.org/10.1017/S026357470500247X Published online by Cambridge University Press

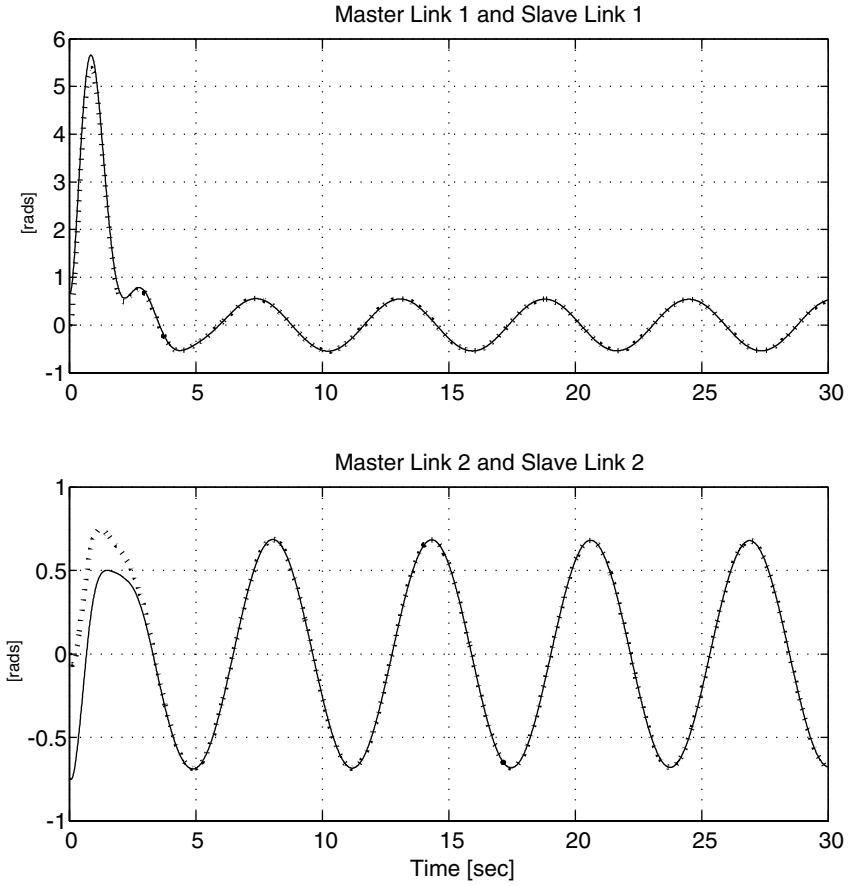

Fig. 7. Actual trajectories for master (i.e. $q_1(t)$) (—) and slave (i.e. $q_2(t)$) (- -) manipulators for Link 1 and Link 2.

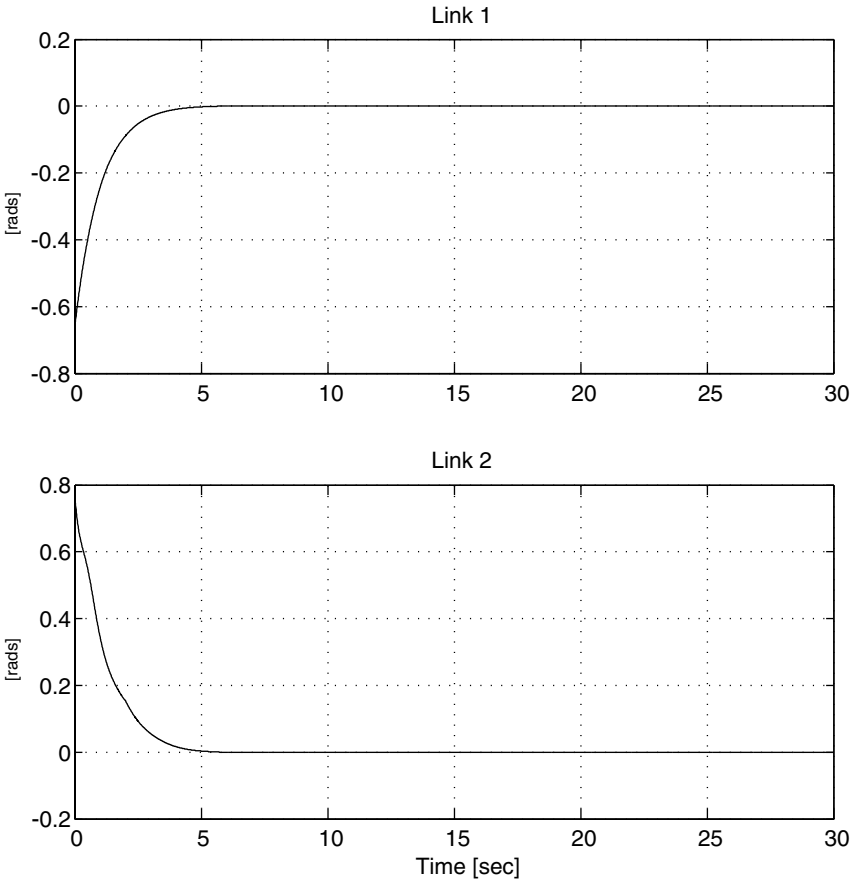

Fig. 8. Link position tracking error between the master and slave manipulators (i.e. $q_1(t) - q_2(t)$).

https://doi.org/10.1017/S026357470500247X Published online by Cambridge University Press

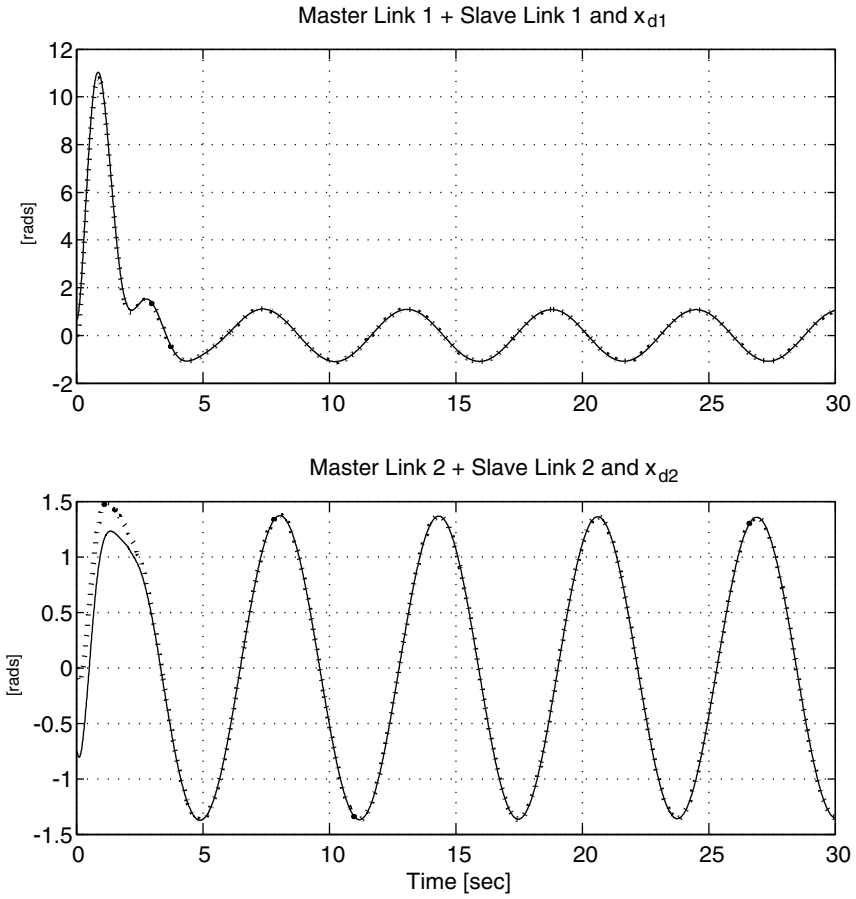

Fig. 9. Actual coordinated (i.e. $q_1(t) + q_2(t)$) trajectory (—) and desired (i.e. $q_d(t)$) trajectory (- -) for Link 1 and Link 2.

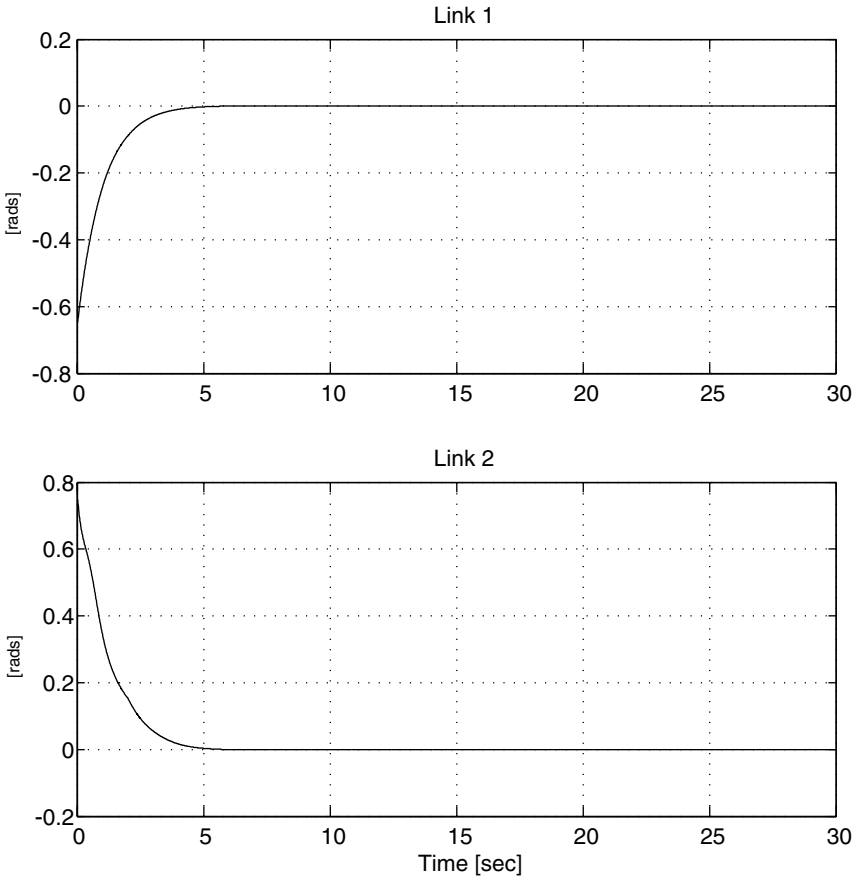

Fig. 10. The coordinated system versus the desired trajectory tracking error (i.e. $q_1(t) + q_2(t) - x_{d2}(t)$).

https://doi.org/10.1017/S026357470500247X Published online by Cambridge University Press

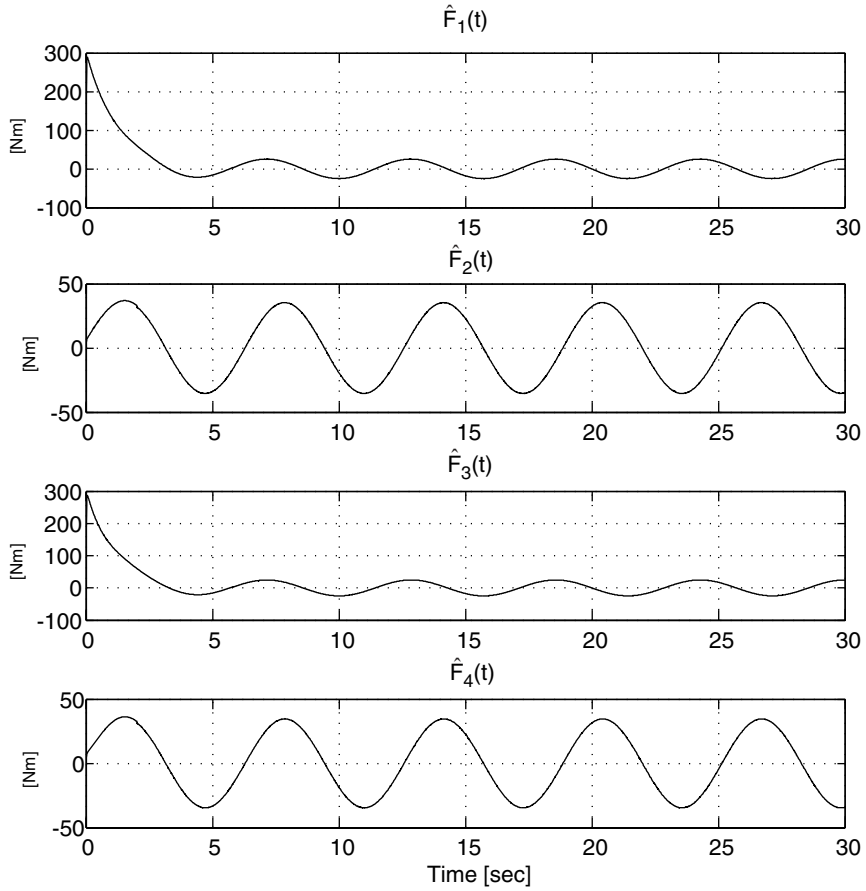

Fig. 11. The output of the nonlinear force observer (i.e. $\hat{F}(t)$).

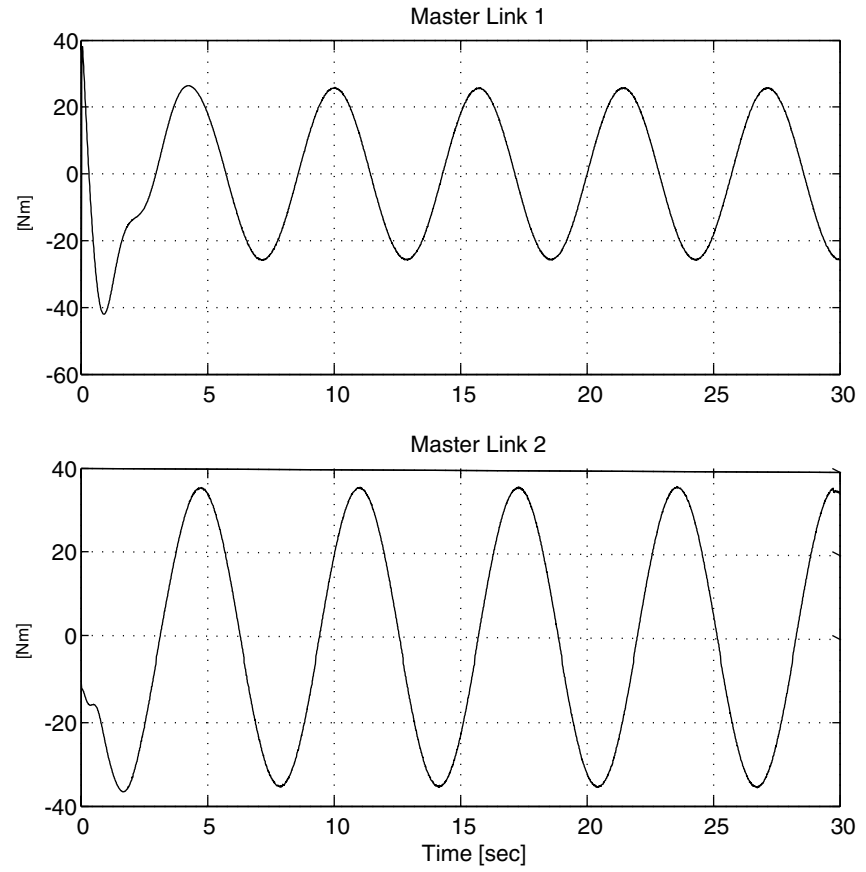

Fig. 12. Master manipulator control input torque (i.e. $\tau_1(t)$).

https://doi.org/10.1017/S026357470500247X Published online by Cambridge University Press

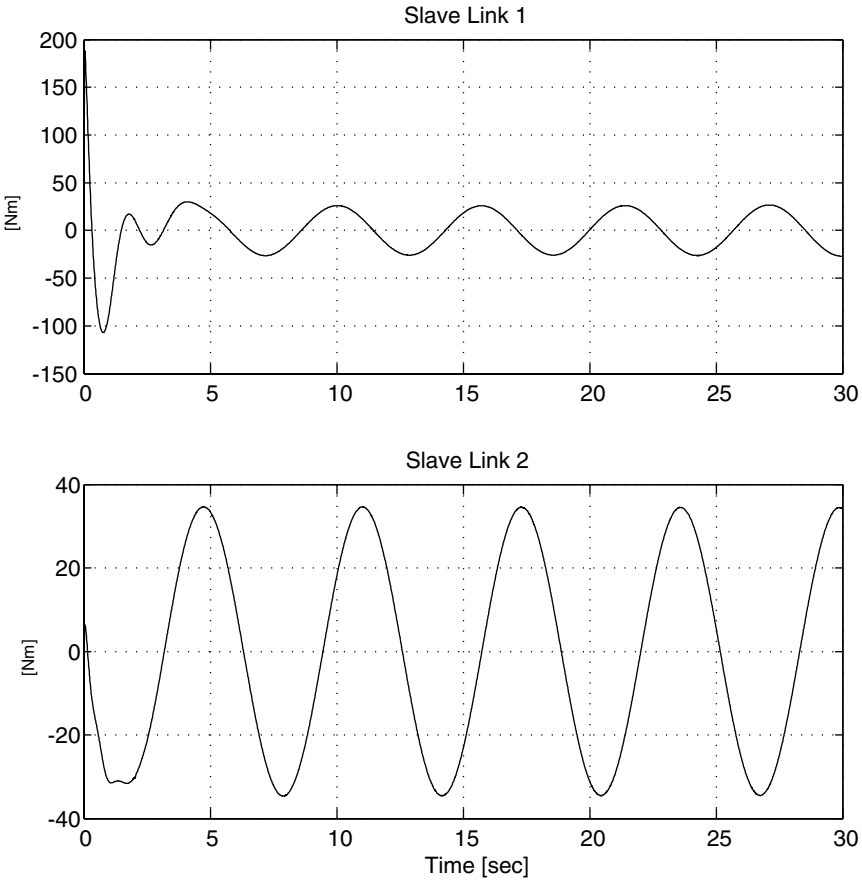

Fig. 13. Slave manipulator control input torque (i.e. $\tau_2(t)$).

is provided in Figure 11. The control torque inputs for both the master and slave manipulators are provided in Figures 12 and 13, respectively.

V. CONCLUSIONS

Through the use of transformations, dynamic trajectory generations, and continuous nonlinear integral feedback terms, two controllers were proven through Lyapunov-based techniques to passively coordinate the master and slave manipulators with respect to the scaled user and environmental power despite incomplete system knowledge. Implementing either controller would provide the user of the closed loop teleoperator system with a power scalable, coordinated master-slave tool that provides safe and stable user feedback. The MIF controller was developed despite uncertainty in the dynamics of the teleoperator system resulting in a semi-global asymptotic result, and the UMIF controller was developed despite unmeasurable user and environmental force inputs resulting in a global asymptotic result. Simulation results demonstrate for both controllers that the coordination and tracking control objectives are met.

References

1. D. Lee and P. Y. Li, "Passive Bilateral Feedforward Control of Linear Dynamically Similar Teleoperated Manipulators," *IEEE Trans. on Robotics and Automation* **19**, No. 3, 443–456 (2003).
2. J. E. Colgate, "Robust Impedance Shaping Telemanipulation," *IEEE Trans. on Robotics and Automation* **9**, No. 4, 374–384 (1993).
3. B. Hannaford, "A Design Framework for Teleoperators with Kinesthetic Feedback," *IEEE Trans. on Robotics and Automation* **5**, No. 4, 426–434 (1989).
4. D. A. Lawrence, "Stability and Transparency in Bilateral Teleoperation," *IEEE Trans. on Robotics and Automation* **9**, No. 5, 624–637 (1993).
5. S. E. Salcudean, M. Zhu, W.-H. Zhu and K. Hashtudi-Zaad, "Transparent Bilateral Teleoperation Under Position and Rate Control," *Int. J. Robot. Res.* **19**, No. 12, 1185–1202 (2000).
6. R. J. Anderson and M. W. Spong, "Bilateral Control of Teleoperators with Time Delay," *IEEE Trans. on Automatic Control* **34**, No. 5, 494–501 (1989).
7. H. Kazerooni and C. L. Moore, "An Approach to Telerobotic Manipulations," *ASME J. Dynam. Syst., Meas., Contr.* **119**, No. 3, 431–438 (1997).
8. H. Kazerooni, T. I. Tsay and K. Hollerbach, "A Controller Design Framework for Telerobotic Systems," *IEEE Trans. on Control Systems Technology* **1**, No. 1, 50–62 (1993).
9. S. E. Salcudean, N. M. Wong and R. L. Hollis, "Design and Control of a Force-Reflecting Teleoperation System with Magnetically Levitated Master and Wrist," *IEEE Trans. on Robotics and Automation* **11**, No. 6, 844–858 (1995).
10. Y. Yokokohji and T. Yoshikawa, "Bilateral Control of Master-Slave Manipulators for Ideal Kinesthetic Coupling – Formulation and Experiment," *IEEE Trans. on Robotics and Automation* **10**, No. 5, 605–620 (1994).
11. N. V. Q. Hung, T. Narikiyo, H. D. Tuan, "Nonlinear Adaptive Control of Master-Slave System in Teleoperation," *Control Engineering Practice* **11**, No. 1, 1–10 (2003).
12. N. Chopra, M. W. Spong, S. Hirche and M. Buss, "Bilateral Teleoperation over the Internet: the Time Varying Delay

https://doi.org/10.1017/S026357470500247X Published online by Cambridge University Press

Problem," *Proc. IEEE American Control Conference*, June 4–6, 2003, Denver, CO (2003), pp. 155–160.
13. N. Chopra, M. W. Spong, R. Ortega and N. E. Barabanov, "On Position Tracking in Bilateral Teleoperators," *Proc. IEEE American Control Conference*, June 30–July 2, 2004, Boston, MA (2004), pp. 5244–5249.
14. D. Lee and P. Y. Li, "Passive Coordination Control of Nonlinear Bilateral Teleoperated Manipulators," *Proc. IEEE Int. Conf. Robotics and Automation*, May 11–15, 2002, Washington, DC (2002), pp. 3278–3283.
15. D. Lee and P. Y. Li, "Passive tool dynamics rendering for nonlinear bilateral teleoperated manipulators," *Proc. IEEE Int. Conf. Robotics and Automation*, May 11–15, 2002, Washington, DC (2002), pp. 3284–3289.
16. B. E. Miller, J. E. Colgate and R. A. Freeman, "Guaranteed Stability of Haptic Systems with Nonlinear Virtual Environments," *IEEE Trans. on Robotics and Automation* **16**, No. 6, 712–719 (2000).
17. G. Niemeyer and J. J. E. Slotine, "Stable Adaptive Teleoperation," *IEEE Journal of Oceanic Engineering* **16**, No. 1, 152–162 (1991).
18. G. Niemeyer and J. J. E. Slotine, "Designing Force Reflecting Teleoperators with Large Time Delays to Appear as Virtual Tools," *Proc. IEEE Int. Conf. Robotics and Automation*, April 20–25, 1997, Albuquerque, NM (1997), pp. 2212–2218.
19. Z. Qu and J.-X. Xu, "Model-Based Learning Controls and Their Comparisons Using Lyapunov Direct Method," *Asian Journal of Control* **4,** No. 1, 99–110 (2002).
20. B. Xian, M. S. de Queiroz and D. M. Dawson, "A Continuous Control Mechanism for Uncertain Nonlinear Systems," *Optimal Control, Stabilization, and Nonsmooth Analysis, Lecture Notes in Control and Information Sciences* (Heidelberg, Germany: Springer-Verlag, 2004), pp. 251–262.
21. F. L. Lewis, D. M. Dawson and C. T. Abdallah, *Robot Manipulator Control: Theory and Practice* (New York, NY: Marcel Dekker, Inc., 2004).
22. M. McIntyre, W. Dixon, D. Dawson and E. Tatlicioglu, "Passive Coordination of Nonlinear Bilateral Teleoperated Manipulators," *Clemson University CRB Technical Report*, CU/CRB/8/16/05/#1, http://www.ces.clemson.edu/ece/crb/publictn/tr.htm.
23. J. J. E. Slotine and W. Li, *Applied Nonlinear Control* (Englewood Cliff, NJ: Prentice Hall, Inc., 1991).

https://doi.org/10.1017/S026357470500247X Published online by Cambridge University Press